

TRANSIENT ECHO FIELD RESULTED BY ULTRASONIC TRANSDUCER WITH ARBITRARY SHAPE APERTURE IN A SOLID

G.G. Lutenco¹, D.V. Galanyenko¹, and V.B. Galanenko¹

¹ Ultracon-Service, Kiev, Ukraine

Abstract: Spatial distribution of echo-signal amplitudes as a function of defect coordinates is computed for ultrasonic transducer with arbitrary shape and for pulse signals of different duration. Such a distribution contains useful information for designing of automatic ultrasonic NDT devices.

For radiation mode the transducer is approximated by external normal tensions which are applied to the surface of an elastic half-space. Transducer integrates normal surface displacements for reception mode. At first, the frequency gain of the “radiation-reflection-reception” process is computed for a specific position of a defect. Then frequency synthesis algorithm is applied and maximal absolute value of the obtained echo-signal is computed. Distribution of this amplitude for various positions of a defect at arbitrary plane section (vertical or horizontal one) gives visual picture of an echo-signal field. Computation of signal spectrum specific frequency is based on two different algorithms. One of them (spatial-spectral algorithm) employs 2D FFT and is applied for small distances within near-field zone. Another algorithm employs spatial convolution procedure and is meant for bigger distances within both near and far field zones.

The echo field structure for transducers with rectangular aperture of the same area and different ratio of sides are computed and discussed. The focusing rectangular transducer echo-field is computed.

Introduction: It is well known that the amplitudes of waves radiated by piezoelectric transducer are distributed non-uniformly in space and echo-signal amplitude depends on reflector position. Temporal gain control can grade undesired amplitude dependence on the coordinate along the acoustical axis of a PET (piezoelectric transducer) but it is not eliminated for all that dependence on transverse coordinate. If a defect is situated within the area of small echo amplitude it may be missed. It is not so important in case manual testing because operator moves the PET in such a manner to find maximal echo-signal. We have different situation when designing automatic system of nondestructive testing since in the case sensors' positions are fixed and defect detection is based on threshold comparison. In this case we should take care to make ultrasonic covering uniform as far as possible. Authors were faced this problem when they were designing the ultrasonic set for nondestructive testing of wagon wheels for testing them during manufacturing. It had served as direct stimulus to undertake investigation which results are presented below.

General view of the radiated field spatial structure in a solid is based on its similarity to the field which radiated by a piston to a liquid. The last one may be computed by means of Kirhgoff-Raleigh integral. However this notion is not sufficient in case it is need of exact quantitative data of spatial amplitude distribution of pulse echo signals. There are a lot of studies [1 - 10] which focused on interference effects which cause time form variation of radiated transient signals for different points of observation. But amplitude spatial distribution is not treated in the referred investigations. The aims of this study are those: 1) to develop appropriate numerical algorithm for computing of the spatial amplitude distribution of echo-signals of arbitrary duration for PETs with arbitrary aperture shape; 2) to apply this algorithm for study of ultrasonic covering area that is defined on such condition: echo-signal amplitude (by dB) from each point situated within the area is allowed to depart from maximal level no more than by definite number of dB.

This computational algorithm is divided into three successive parts: computation of radiated field, computation of the field reflected by the obstacle and computation of the signal at PET electrical output. Getting of exact solutions of these problems is very difficult. So we are forced to resort to essential simplifications but trying to retain most important factors which determine spatial structure of echo-signal field. For example exact formulation for radiated field computation involves considering of joint motion of elastic half space and all the elements of the moving assembly of a PET caused by pulse signal at electrical input. It is not only intractable problem but it requires specification of the PET construction every time. At the same time field spatial structure is determined in the main by spatial distribution of a PET impact to the medium at the contact area and weakly depends on the parameters of PET construction. So, following to the many authors [1 - 10] we replace exact mathematical formulation of the problem (as a contact one) by approximate boundary problem in which action of the PET to the elastic medium is approximated by normal tensions applied to its surface. In analogous way the spatial filtration of the signal field by

extended PET aperture is governing factor under receive mode. Let us suppose that output signal is proportional to the integral of normal displacements over PET aperture. In fact such approximations separate two kinds of signal time filtration: by resonant moving assembly of a PET and spatial-time filtration during radiation, propagation and receiving. In this case echo-signal output spectrum may be presented as product of the input electrical signal spectrum by three factors: frequency gain of the PET in radiate mode, its frequency gain in receive mode and so called acoustical frequency gain

$$S_{out}(\omega, \mathbf{x}) = S_{in}(\omega)K_{rad}(\omega)K_{rec}(\omega)K_{ac}(\omega, \mathbf{x}) \quad (1)$$

where \mathbf{x} is coordinate vector of the scatterer central point.

As PET frequency gains for radiate and receive modes are well studied, for initial spectrum we specified spectrum of the signal having already been filtrated by PET under receiving and radiation:

$$S_0(\omega) = S_{in}(\omega)K_{rad}(\omega)K_{rec}(\omega) \text{ (ore corresponding signal time form } S_0(t) \text{), see. fig. 1 as an example.}$$

The main part of the computation procedure is computing of acoustical frequency gain for all frequencies of signal spectrum. When $K_{ac}(\omega, \mathbf{x})$ is obtained the echo-signal form in time domain is computed by frequency synthesis method as follows:

$$s(t, \mathbf{x}) = 2 \operatorname{Re} \left(\int_0^{\infty} S_0(\omega) K_{ac}(\omega, \mathbf{x}) \exp(-i\omega t) d\omega \right) \quad (2)$$

Function $A(\mathbf{x}) = \max(\operatorname{abs}(s(t, \mathbf{x})))$ describes spatial structure of echo-signal field. It is ultimate aim of the computation.

Results: We are coming now to computation of the field scattered by a defect that is important part of acoustical frequency gain computation. We use hollow half-cylinder with a flat bottom as a standard model of a defect. As the surface of this scatterer is free of stresses one can present displacement vector of scattered field as follows:

$$\mathbf{u}_r(\mathbf{x}, \omega) = - \int_S \boldsymbol{\sigma}_i(\mathbf{x}') \mathbf{G}_1(\mathbf{x}, \mathbf{x}') dS' \quad (3)$$

where $\boldsymbol{\sigma}_i(\mathbf{x}')$ is stress vector for incident wave at the scatterer surface, $\mathbf{G}_1(\mathbf{x}, \mathbf{x}')$ is Green's displacement tensor for isotropic elastic space with the cylindrical hollow. In contrast to Green's tensors for free space (see [11]) this tensor is unknown. So, expression (3) is unsuitable for direct computation. However it can be useful for simplified computation ground (because exact solution of this diffraction problem is unknown).

If the scatterer is situated within alight zone incident, wave direction is not as strongly apart from the cylinder axis. Then the part of scattered field which is connected with side cylinder surface is expected to run almost along cylinder axis (like a wave radiated by traveling-wave antenna). Income of this part into echo-signal is supposed to be negligible. Then the scatterer is similar to the round piston with soft cylindrical screen which screens piston underside. Let us replace cylindrical screen by plane one. Although such replacement changes radiation conditions (excitation of a surface wave changes; radiation into whole space angle is replaced by radiation into hemisphere) it is supposed that such approximation is suitable for the analysis of echo-field spatial structure. This situation is analogous to that in acoustics when half-piston is replaced by piston with flat screen.

Let us suppose that all these approximations are allowable. Then order of computations looks like follows. By using of known solution of Lamb's problem which based on two-dimensional Fourier transform we compute normal and tangential stresses at flat bottom of the scatterer for incident (radiated) compression wave. Then we use the same algorithm for computing scattered field and calculate normal displacements at the PET aperture. After integration over aperture we find the amplitude of output signal harmonic component and can use expression (2).

We have most simple relationships when reflector diameter is so small that variation of incident wave amplitude is negligible at its surface. Then:

$$K_{ac}(\omega, \mathbf{x}) = s_b K_{\sigma_i}(\omega, \mathbf{x}) K_{i_w}(\omega, \mathbf{x}) \quad (4)$$

Here: s_b - square of the half cylinder bottom; repeating indices mean summation ($i = 1, 2, 3$).

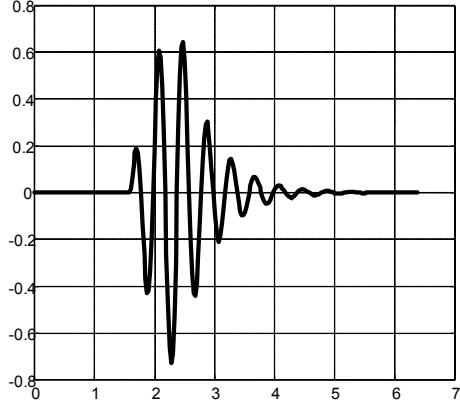


Fig.1. Typical pulse form used under computing.

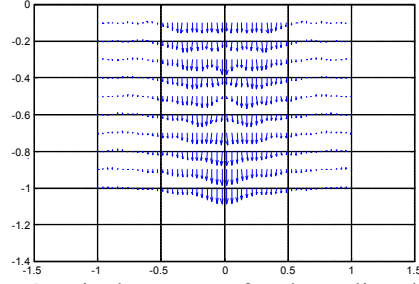


Fig. 2. Displacements for the radiated field (PET diameter $D=12\text{ mm}$, $f_0=5\text{ MHz}$). Vertical coordinate is normalized to near zone length, horizontal one – to the diameter)

$$K_{\sigma i} = \int_{-\infty}^{\infty} \int_{-\infty}^{\infty} S_1(\alpha, \beta) F_1(\kappa) b_{\sigma i} \exp(-\gamma_l z) \exp(i(\alpha x + \beta y)) d\alpha d\beta \quad (5)$$

$$\begin{Bmatrix} K_{1w} \\ K_{2w} \\ K_{3w} \end{Bmatrix} = \int_{-\infty}^{\infty} \int_{-\infty}^{\infty} S_2(\alpha, \beta) \begin{Bmatrix} -\alpha/\kappa F_1(\kappa) \\ -\beta/\kappa F_1(\kappa) \\ F_2(\kappa) \end{Bmatrix} \gamma_l \exp(-\gamma_l z) \exp(i(\alpha x + \beta y)) d\alpha d\beta \quad (6)$$

$S_1(\alpha, \beta)$ и $S_2(\alpha, \beta)$ are Fourier transforms of sensitivity distribution over PET aperture for radiate and receive modes, respectively; $F_1(\kappa) = (k_s^2 - 2\kappa^2)/D$; $F_2 = 2i\kappa\gamma_s/D$; $\kappa = \sqrt{\alpha^2 + \beta^2}$; $\gamma_s^2 = \kappa^2 - k_s^2$; $\gamma_l^2 = \kappa^2 - k_l^2$; k_s, k_l - wave numbers of shear and longitudinal waves; $\mathbf{b}_{\sigma} = \{2i\alpha\gamma_l, 2i\beta\gamma_l, (k_s^2 - 2\kappa^2)\}$; $D = (k_s^2 - 2\kappa^2)^2 - 4\kappa^2\gamma_s\gamma_l$. Written above expressions describe compression component of the wave field. Part of which corresponds to Raleigh surface wave. Integrand singularity at $\kappa = k_R$ which complicates computation corresponds to Raleigh wave income. It is necessary modify expressions determining F_1 and F_2 (using known theorem for meromorphic functions) and replace them by following expressions

$$\tilde{F}_1 = F_1 - \frac{2ik_R\gamma_s}{D'(k_R)} \left(\frac{1}{\kappa - k_R} + \frac{1}{\kappa + k_R} \right); \quad \tilde{F}_2 = F_2 - \frac{k_s^2 - 2k_R^2}{D'(k_R)} \left(\frac{1}{\kappa - k_R} - \frac{1}{\kappa + k_R} \right)$$

Expressions (5) and (6) with fixed value of z can be treated as Fourier transforms of the spatial spectra which vary with depth. Two-dimensional FFT occurs to be convenient numerical algorithm for practical computations. Algorithm FFT applied once gives spatial distribution over plane at fixed depth. We get spatial picture by repeating computations for sequence of depths.

“Spectral” algorithm presented above can become ineffective at big values of z because of factor $f_2(\kappa) = \exp(-\gamma_l z)$ oscillates in integrands of expressions (5) and (6). Different algorithm (named “convolutional” one) is expected to be more convenient for this case. Let us treat factor $f_2(\kappa)$ and preceding part of the integrand (denoted here by $f_1(\alpha, \beta)$) as 2D spectrums of some functions of spatial variables $q_2(x, y)$ and $q_1(x, y)$ respectively. As function $q_2(x, y, z)$ describes the field of an acoustical dipole at fixed depth

$$q_2(x, y) = \frac{z}{r} \frac{ikr - 1}{r} \left(\frac{1}{r} \exp(ikr) \right); \quad r = \sqrt{x^2 + y^2 + z^2}$$

it is expedient to compute expressions (5) and (6) as convolution of $q_2(x, y)$ and $q_1(x, y)$. But due to improper asymptotic behavior of $f_1(\alpha, \beta)$ respective Fourier integral is diverged. So convolution theorem can be applied to Fourier transforms of modified functions $f_1(\kappa) \exp(-\gamma_l z_0)$ and $\exp(-\gamma_l(z - z_0))$. With reference to expression (5) function $q_1(x, y, z_0)$ presents radiated field at depth z_0 and $q_2(x, y, z_0)$ is field of a dipole located at the plane $z = z_0$. Respective convolution integral is analogous to the Kirhgoff-Raleigh integral for a flat acoustical source and differs from the above in that the dipole amplitudes are proportional to values at distant plane $z = z_0$ but not to values at source surface (in practice z_0 may be equal a part of wavelength).

For big values of depth z (in far acoustical zone) it is easy matter to compute convolution integral by using simplifications which are typical for Fraunhofer zone. It leads to expressions for directivity patterns per function $f_1(k_l \sin \theta \cos \varphi, k_l \sin \theta \sin \varphi)$, where θ, φ are spherical angles.

Discussion: Let us consider some computations by means of above algorithms. One can see from Fig. 2 that displacements respected to radiated field are almost parallel to vertical axis (so to the axis of half-cylinder scatterer). It justifies above approximations partially.

First of all let us concern with time form of echo-signals. Shoch (see [12]) was probably the first who predicted that transient signal radiated by a round piston into liquid breaks down into two parts which can be distinct in time. This effect is also observed in a solid. Most clear investigation for signals radiated into solid can be found in Refs. [5 – 7]. It can be expected that “Shoch effect” takes place when we deal with echo-signals. We are going to illustrate this effect by computing of echo-signals reflected by a small scatterer located at the axis of a PET.

We approximated initial pulse form as follows

$$s_0(t) = t^b \exp(-\beta t) \sin(\omega_0 t) \text{ with the spectrum}$$

$$S(\omega) = \frac{\Gamma(b+1)}{2i} (U_1(\omega) - U_2(\omega))$$

$$U_{1,2}(\omega) = \left((\beta \mu i \omega_0)^2 + \omega^2 \right)^{-(b+1)/2} \exp\left(i(b+1) \arctg\left(\frac{\omega}{\beta \mu i \omega_0} \right) \right)$$

Echo-signals scattered by obstacle at different depths and received by transducer with round aperture are illustrated by Fig. 3.

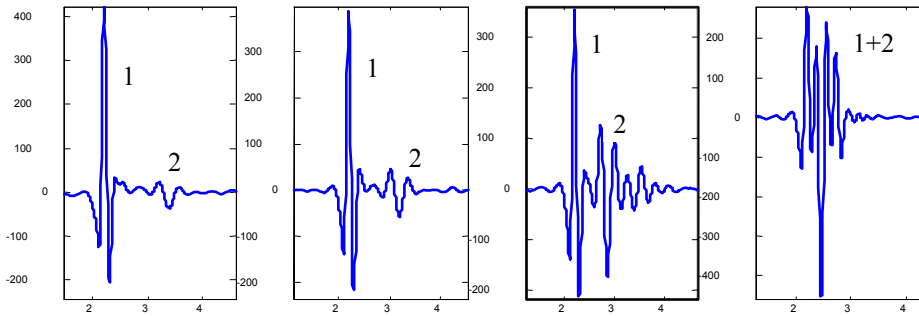


Fig. 3. Echoes from $z=3, 5, 10, 30$ mm (from left to right). The abscissa is the time by mcs with removed travel interval. Diameter $D=20$ mm, $f_0=5$ MHz, $c_l=6000$ m/s, $c_s=3240$ m/s.

According to Shoch approach (modified for solids [5]) radiated field consists of direct plane compression wave (1), compression edge wave (2), shear and head edge waves. One can see two first of them at Fig. 3.

As this effect results from wave interference it must depend on aperture form. Really the effect is not so significant for transducer with square aperture (Fig. 4).

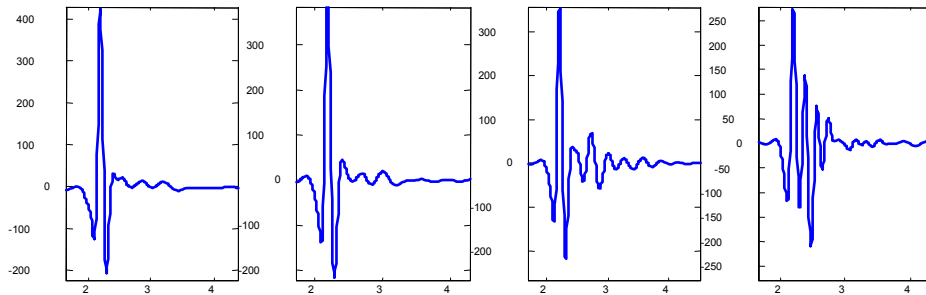


Fig. 4. Echoes from $z=3,5,10,30$ mm (from left to right). Square aperture 20×20 mm, $f_0=5$ MHz, $c_l=6000$ m/s, $c_s=3240$ m/s.

Let us consider spatial structure variation of echo field with variation of piezoelectric plate form.

One can see from Fig. 5 that redistribution of amplitude between interference maxima is exhibited with the plate width decreasing: maximal amplitude values migrate from central axis to side zones and come near the plate.

Echo field structure is closely connected with AVG-diagrams which are widely used in NDT practice [13]. They present echo-signal level as function of two normalized variables. One of them – distance - is normalized by the length of near acoustical zone that is usually determined as follows: $L_{nz} = a^2 / \lambda = S / \pi \lambda$, where a

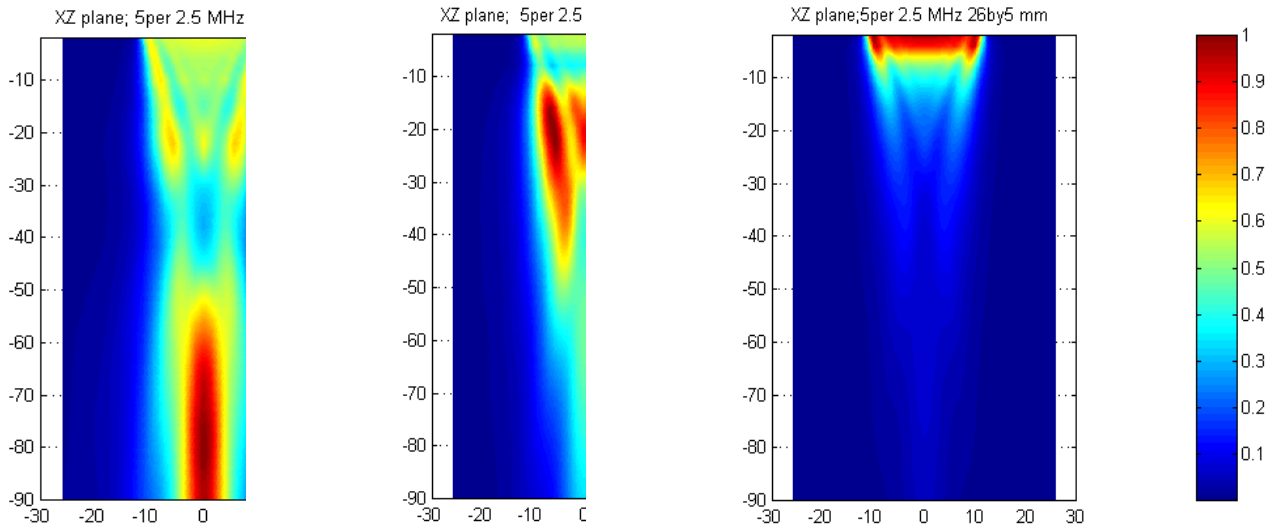


Fig. 5. Amplitude spatial distribution for plates of different size: 26×26 mm, 26×13 mm and 26×5 mm at 2.5 MHz. Pulse form is the same like shown at Fig.1 (duration: 5 periods). Abscissa and ordinate are distances by mm.

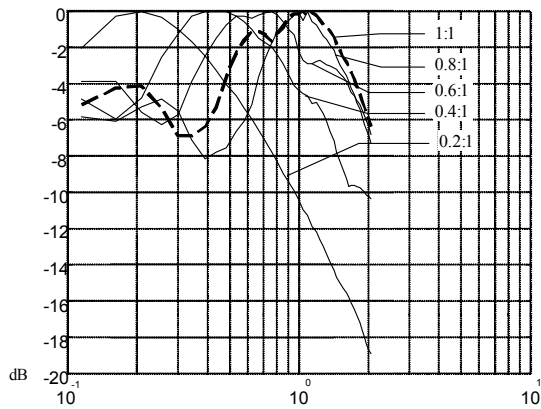


Fig. 6. Maximal amplitude dependence on longitudinal coordinate normalized to L_{mz} for transducers with rectangular aperture and with different side ratio of the rectangle.

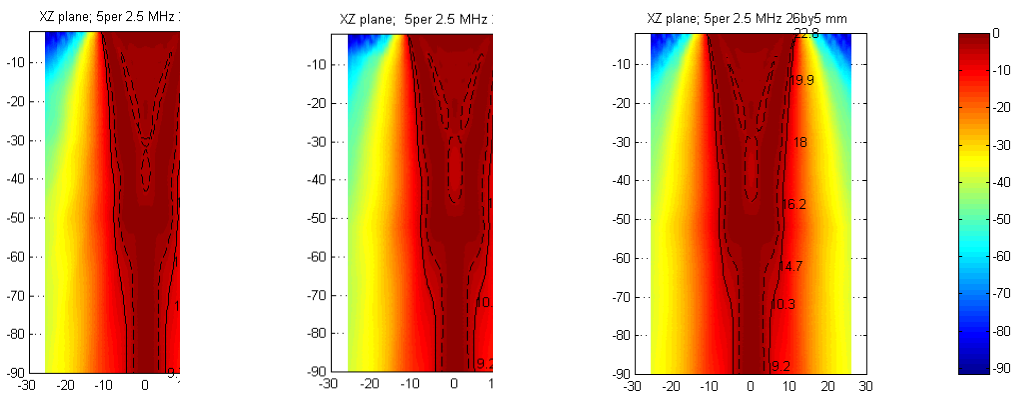


Fig. 7. Amplitudes (by dB) normalized to maximal value at current depth for plates of different size: 26×26 mm, 26×13 mm, 26×5 mm at 2.5 MHz. Level of -6 dB is shown by solid line, dashed line marks the level of -3 dB. Labels mark width of “-6 dB zone” by mm at current depth.

is the radius of a circle which is equal-squared to the transducer aperture. The value of $z = L_{nz}$ is characteristic point at longitudinal axis of a transducer: signal level decreases monotonically beginning from this point. Let us consider maximum position of the function $A_{\max}(z)$ for rectangular aperture with constant square and varying side ratio. Rectangular plate with square equal 324 mm^2 , working frequency 2.5 MHz and pulse duration of 2 mcs was used for computation amplitude level in steel. Plate form varied from the square ($18 \times 18 \text{ mm}$) to the rectangle with side ratio equal 5:1. Fig. 6 demonstrates that maximum position comes near the aperture with disproportion increase. It seems that one can use standard AVG-diagrams for rectangular transducers while side ratio is no less than 0.8:1.

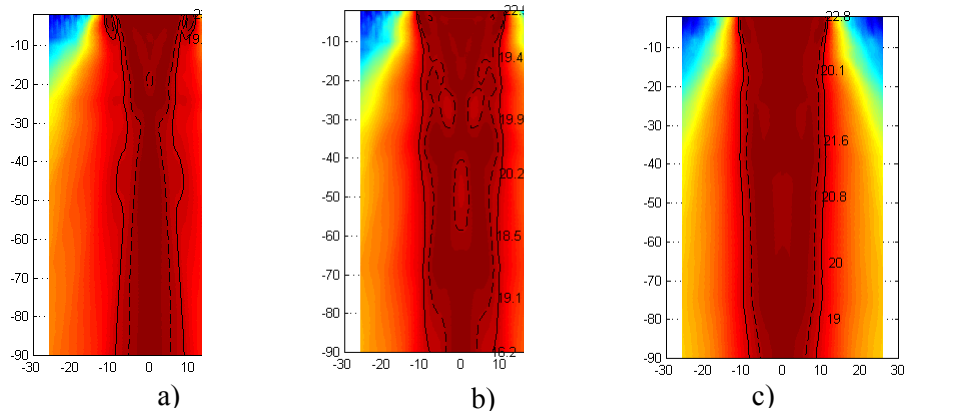


Fig. 8. Normalized amplitude distribution (by dB) for 3-element array ($3 \times 14 \text{ mm} + 20 \times 10 \text{ mm} + 3 \times 14 \text{ mm}$) with different amplitude-phase sensitivity distribution over elements (a) and b) – pulse duration is 5 periods, c) – 2 periods; solid line marks level of -6 dB, dashed line - -3 dB).

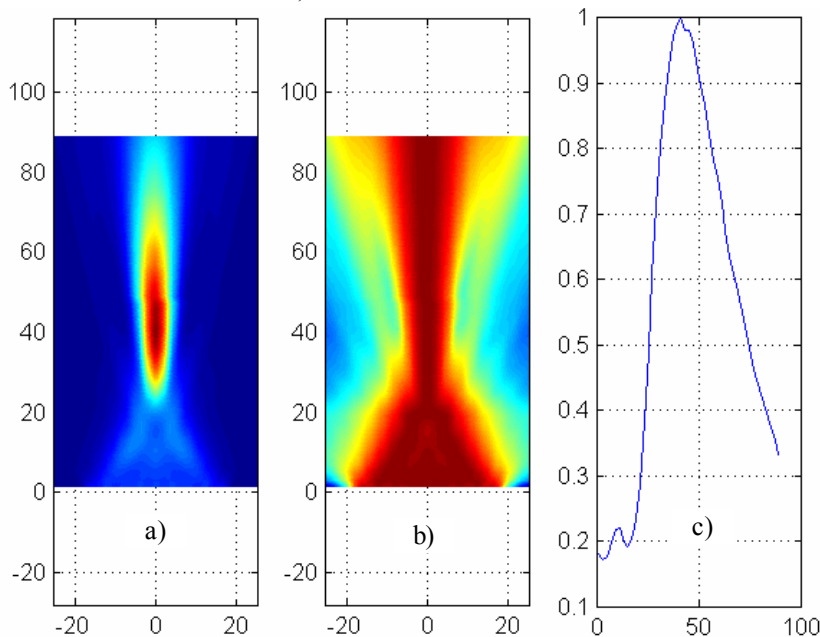


Fig. 9. Echo-field structure for 9-element focusing array. First picture corresponds to unnormalized spatial distribution, second one describes field normalized to maximal amplitude at current depth and represented by dB. In the third window $A(z)$ is shown.

Let suppose that time control of amplification factor that is applied in receive mode allows to normalize the signal level to maximal amplitude at current depth. Spatial distribution of normalized signal amplitude

$N(x, z) = 20 \lg(A(x, z)/\max(A(z)))$ is shown at Fig. 7. Level lines at Fig. 7 can be treated as the border of alight zone. Undesirable features of these zones are those: width of the alight zone may be substantially less than the plate width, there are holes in the middle of alight zone. Situation may make a little better by using 3-element array with respectively picked amplitude-phase distribution for receive mode (Fig. 8). As expected, spatial amplitude distribution became more equable with decreasing of pulse duration.

Above discussed numerical algorithm may be applied to computing of field structure of multielement phased arrays. Fig. 9 demonstrates an example of such computation. Array consisted of nine elements of size 30×3 mm with the gap of 1 mm between them; working frequency is 1 MHz, pulse duration is equal to 5 cycles. Amplitude-phase distribution of sensitivity over elements is that to focus array to the point at distance 45 mm along longitudinal axis within steel specimen. As it can be seen amplitude maximum is reached at the focus point (Fig. 9 a, c). But if time control of amplification factor is applied to normalize the signal to maximal amplitude at current depth the most narrow cross-section of alight zone is situated at $z=35$ mm. Diameter of this cross-section (by level -6 dB) is equal to 6 mm.

Conclusions: Time and spatial structure of echo-field depends on aperture geometry, working frequency of the transducer, pulse duration and on law upon which time control of amplification factor is based. Considered computational algorithm allows studying this structure in a wide range of parameters.

References: 1. K. Kawashima. Theory and numerical calculation of the acoustical field produced in metal by an electromagnetic ultrasonic transducer. Journ. Acoust. Soc. Am., 1976, **60**, No. 5, p. 1089-1099.

2. X. M. Tang, M. N. Toksoz, C. H. Cheng. Elastic wave radiation and diffraction of a piston source. Journ. Acoust. Soc. Am., 1990, **87**, p. 1894 – 1902.

3. Bresse L.F., Hutchins D.A. [Transient Generation of Elastic Waves in Solids by a Disk-shaped Normal Force Source](#). Journ. Acoust. Soc. Am., 1989, **86**, p. 810 – 817.

4. K. Kawashima. Quantitative calculation and measurement of longitudinal and transverse wave pulses in solid. IEEE Transactions, Sonics Ultrasonics, SU-31, 1984, p. 83-94.

5. Dielouah H., Baboux J.C. [Transient Ultrasonic Field Radiated by a Circular Transducer in a Solid Medium](#). Journ. Acoust. Soc. Am., 1992, **92**, p. 2932 - 2941.

6. Baboux J.C., Kazys R. Analysis of the [transient ultrasonic fields radiated in solids by a circular and annular sources](#). Journ. Acoust. Soc. Am., 1992, **92**, p. 2942 - 2951.

7. Kazys R., Baboux J.C. [Transient Radiation of Ultrasonic Waves in Solids by Nonuniformly Excited and Focusing Annular Arrays](#). Journ. Acoust. Soc. Am., 1992, **92**, p. 2952 – 2960

8. McNab A., Cochran A., Campbell M.A. [The Calculation of Acoustic Fields in Solids for Transient Normal Surface Force Sources of Arbitrary Geometry and Apodization](#). Journ. Acoust. Soc. Am., 1990, **87**, p. 1455 – 1465.

9. Schmerr L.W., Jr., Sedov A. [An Elastodynamic Model for Compressional and Shear Wave Transducers](#). Journ. Acoust. Soc. Am., 1989, **86**, p. 1988 – 1999.

10. Lhemery A. [A model for the transient ultrasonic field radiated by an arbitrary loading in a solid](#). Journ. Acoust. Soc. Am., 1994, **96**, p. 3776-3786.

11. Yih-Hsing Pao, Vasundara Varatharajulu. Huygens' principle, radiation conditions, and integral formulas for the scattering of elastic waves. Journ. Acoust. Soc. Am., 1976, **59**, p. 1361 – 1371.

12. G. R. Harris, Review of [transient field theory](#) of baffled planar piston. Journ. Acoust. Soc. Am., 1981, **70**, p. 10-20.

13. Josef Krautkramer, Herbert Krautkramer. Werkstoffprüfung mit Ultraschall. Springer-Verlag, Berlin, 1986